Chinese Journal of Aeronautics, (2017), 30(3): 1184–1195

Chinese Society of Aeronautics and Astronautics
& Beihang University

Chinese Journal of Aeronautics

cja@buaa.edu.cn
www.sciencedirect.com

Air route network optimization in fragmented airspace based on cellular automata

Shijin WANG [a], Xi CAO [a], Haiyun LI [a], Qingyun LI [a], Xu HANG [b], Yanjun WANG [a,*]

[a] *College of Civil Aviation, Nanjing University of Aeronautics and Astronautics, Nanjing 210016, China*
[b] *Air Traffic Control Division, Central-south Regional Air Traffic Management Bureau, Guangzhou 510405, China*

Received 18 May 2016; revised 18 September 2016; accepted 27 November 2016
Available online 26 April 2017

KEYWORDS

Air route network planning;
Airspace restriction;
Cellular automata;
Network capacity;
Optimization of nodes

Abstract Air route network optimization, one of the essential parts of the airspace planning, is an effective way to optimize airspace resources, increase airspace capacity, and alleviate air traffic congestion. However, little has been done on the optimization of air route network in the fragmented airspace caused by prohibited, restricted, and dangerous areas (PRDs). In this paper, an air route network optimization model is developed with the total operational cost as the objective function while airspace restriction, air route network capacity, and non-straight-line factors (NSLF) are taken as major constraints. A square grid cellular space, Moore neighbors, a fixed boundary, together with a set of rules for solving the route network optimization model are designed based on cellular automata. The empirical traffic of airports with the largest traffic volume in each of the 9 flight information regions in mainland China is collected as the origin-destination (OD) airport pair demands. Based on traffic patterns, the model generates 35 air routes which successfully avoids 144 PRDs. Compared with the current air route network structure, the number of nodes decreases by 41.67%, while the total length of flight segments and air routes drop by 32.03% and 5.82% respectively. The NSLF decreases by 5.82% with changes in the total length of the air route network. More importantly, the total operational cost of the whole network decreases by 6.22%. The computational results show the potential benefits of the model and the advantage of the algorithm. Optimization of air route network can significantly reduce operational cost while ensuring operation safety.

1. Introduction

In the period of 2011 to 2015, the average annual growth rates of the number of operations at the airport (in terms of takeoff and landing) and passenger throughput have reached to 9.4% and 10.2% respectively. It is foreseen that air transport in China will continue to grow at a high rate. The number of air-

* Corresponding author.
E-mail address: ywang@nuaa.edu.cn (Y. WANG).
Peer review under responsibility of Editorial Committee of CJA.

http://dx.doi.org/10.1016/j.cja.2017.04.002
1000-9361 © 2017 Chinese Society of Aeronautics and Astronautics. Production and hosting by Elsevier Ltd.

craft in 2020 is predicted to reach 4600, while the number of civil airports will be 270. By 2025, the global air traffic will continue to increase with an annual rate of 3%.[1] The rapid growth of air traffic demand will lead to serious problems in the air transportation system, such as airspace congestion, flight delay, etc. The effective utilization of air route network (ARN) resources is fundamental to solve these problems.

ARN is constructed by fixed nodes (including airports and boundary nodes), air route network nodes (ARNNs), and air routes. The spatial distribution and quantity of ARNNs determine the position, direction, segment lengths of the route segments, as well as air route network security elements. ARN plays an important role in transporting passengers and cargo.

Research in air traffic network mainly focuses on two aspects: complex analysis of airport network topology, and optimization of ARN topology structure.[2–4] Du et al.[2] have analyzed the Chinese airline network (CAN) as multi-layer networks and investigated its robustness. Cao et al.[4] have studied the topology structure of Chinese ARN and CAN based on complex network metrics such as average degree, average shortest path length, and clustering coefficient. A directed air-route network topology evolution method was proposed by Zhao et al.[5] for designing airspace to test ARN structure optimization. By merging and moving nodes, ARN costs are minimized under traffic control constraints. Based on a mesh fabric, Rivière[6] employed shortest path algorithm to optimize ARN. Cai et al.[7] developed a bi-level objective model and a memetic algorithm with push-pull operator to improve the evaluation indices. Optimization algorithms were developed for improving network capability, such as particle swarm optimization.[8,9] Jin et al.[10] built a multi-objective ARN optimization model based on ARN capacity, flight efficiency, and airspace safety, and proposed a multi-objective optimization algorithm based on comprehensive learning of particle swarm optimization and the Floyd-Walsh algorithm to solve the model. Chen[11] developed an ARN traffic flow model by proposing a single-objective particle swarm algorithm based on a betweenness guide and introducing a multi-objective particle swarm optimization algorithm for ARN capacity.

There are many prohibited, restricted, and dangerous areas (PRDs) in airspace, which makes ARN environment "fragmented". Fig. 1 shows PRDs in airspace in mainland China. Grey areas represent PRDs which are the major constraints for ARN optimization. Areas outside the grey areas can be used, which means that the available air-route network optimization space is discontinuous. Thus, PRDs must be considered when ARN is optimized. However, all the work mentioned above did not consider the fragment airspace environment. Zhao et al.[5] proposed a model based on the MAKLINK Graph method, using a multi-objective genetic algorithm based on fast non-dominated sorting to find solutions which avoids PRDs. Due to the limitations of the MAKLINK Graph method, it is applicable only to "convex" PRDs. Xu and Zhu[12] used a genetic algorithm to solve the ARN optimization model considering PRDs. The algorithm is however time-consuming. Wang and Gong[13] developed an ARN optimization model which avoids PRDs and introduced a new algorithm based on cellular automata (CA). The model comprehensively considered flight safety and cost constraints to optimize path length. In this work, it ignored segment traffic flows, focusing only on path length. Neither work described here considered ARN capacity, which could result in airspace congestion.

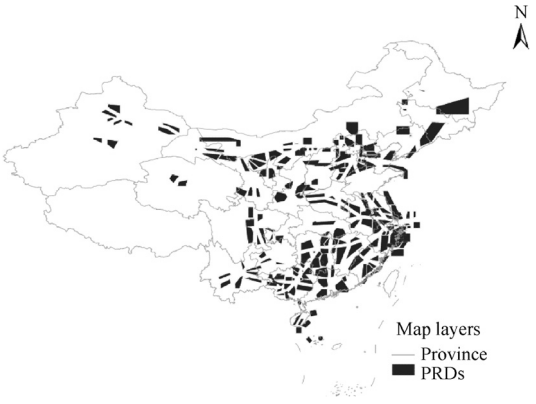

Fig. 1 Illustration of PRDs in China (PRDs are marked with grey).

This paper aims to optimize ARN structure in fragmented airspace. The objective is to minimize total operational cost. An ARN optimization model is developed considering constraints on different node configurations of ARN capacity, non-straight-line factors (NSLF), and the range of mobility of ARNNs boundaries. A CA based algorithm is proposed to solve the model. To test the model, traffic flow of airports with the largest flow in each of the 9 flight information regions (FIR) is used as origin-destination (OD) demand. Computational results show the benefits of the model and the advantage of the algorithm.

2. ARN capacity model

ARN capacity is defined as the capability of an ARN to accommodate air traffic flow. ARN capacity can be divided into node capacity and segment capacity given certain conditions of airspace system structure, security restrictions, and operation regulations. At the design phase of an ARN, the following assumptions are made to investigate ARN capacity:

(1) An aircraft flies at a constant speed, and all aircraft have the same speed.
(2) Aircraft can be seen as a particle which flies along the center line of its route.
(3) Only the aircraft flying in the same direction in the same flight level are considered; horizontal separation must be maintained between flights.
(4) Continuous flow of aircraft is waiting to enter the route.

2.1. Route segment capacity

The route segment capacity C_s can be expressed as

$$C_s = 1/T_c \tag{1}$$

where T_c is the time interval between two consecutive aircraft. In average-speed model, let v be the average speed for all aircraft, L_d be the distance between two consecutive aircraft, and L_{min} be the minimum safety separation, and then we have

$$T_c = L_d/v \tag{2}$$

To ensure safety, the distance between aircraft must be larger than the minimum separation. To obtain the largest route segment capacity, we have

$$T_{\min} = L_{\min}/v, \quad C_{\text{smax}} = 1/T_{\min} \tag{3}$$

2.2. ARNN optimization model

ARNNs can be categorized according to flying directions, including converging, diverging, turning, and crossing (Fig. 2). In the figure, α is the convergence angle, β is the divergence angle, while θ and γ is the turning angle. Given different angles of α and β, one can have different traffic status.

(1) If $\alpha = 0$ and $\beta \neq 0$, the crossing flying model is transferred into a converging flying model (Fig. 2(b)).
(2) If $\alpha \neq 0$ and $\beta = 0$, the model is a diverging flying model (Fig. 2(c)).
(3) If $\alpha = 0$ and $\beta = 0$, the model is a turning flying model (Fig. 2(d)).
(4) If $\alpha \neq 0$ and $\beta \neq 0$, the model is a crossing flying model (Fig. 2(e)).

Converging, diverging, and turning flying between routes are special cases of a crossing flying. There are certain amount of research work on these flying models.[14,15] Here, the following two cases are analyzed.

2.2.1. Crossing route

As shown in Fig. 3, OP_s and ON_s are converging route segments, and OQ_s and OM_s are diverging route segments. Suppose there are two aircraft A and B, and A will cross intersection node O after B (Fig. 3). Let x denotes the horizontal distance between the two aircraft, L_D denotes the length of segment OI_s, and t represents the flying time. When $t = 0$, B is at O and A is at I_s. When $t > 0$, if A does not pass O, for instance A and B are at H_s and K_s respectively, then x can be calculated as

$$x = \sqrt{(L_D - vt)^2 + (vt)^2 - 2(L_D - vt) \times vt \times \cos\theta} \tag{4}$$

If A has already crossed O, say if A and B are at M_s and Q_s, then x can be obtained by

$$x = \sqrt{(vt - L_D)^2 + (vt)^2 - 2(vt - L_D) \times vt \times \cos\beta} \tag{5}$$

When $t < 0$, A and B are at P_s and N_s. x is described by

$$x = \sqrt{(L_D - vt)^2 + (-vt)^2 - 2(L_D - vt) \times (-vt) \times \cos\alpha} \tag{6}$$

For each case, one can have the minimum aircraft release time interval $T_{\min}$. Finally we will gain the node capacity $C_n = 1/T_{\min}$.

If A crossed O before B, the same method can be used based on Fig. 3(b). The capacity of node O is therefore given by

$$C_n = \max\left(\max\left(\frac{v}{L_{\min}\sqrt{\frac{2}{1-\cos\theta}}}, \frac{v}{L_{\min}\sqrt{\frac{2}{1-\cos\beta}}}\right), \max\left(\frac{v}{L_{\min}\sqrt{\frac{2}{1-\cos\gamma}}}, \frac{v}{L_{\min}\sqrt{\frac{2}{1-\cos\beta}}}\right)\right) \tag{7}$$

2.2.2. Multiple crossing routes

As shown in Fig. 4(a), there are u air routes, namely R_1, $R_2, \ldots, R_u$, converging to a single route. The capacity of the merging node is $\max(C_{\text{ncon1}}, C_{\text{ncon2}}, \cdots, C_{\text{nconω}})$, $(\omega = C_u^2)$. There are p routes (S_1, $S_2, \ldots, S_p$) diverging at a node are shown in Fig. 4(b). The capacity of the node is $\max(C_{\text{ndir1}}, C_{\text{ndir2}}, \ldots, C_{\text{ndirτ}})$, $(\tau = C_p^2)$. As depicted in Fig. 4 (c), u routes converge at a node and then diverge into p routes. In this case, the capacity of intersection node is $\max(C_{\text{ncro1}}, C_{\text{ncro2}}, \cdots, C_{\text{ncroq}})$, $(q = \omega\tau)$.

3. ARN optimization model

To build the ARN optimization model, the following assumptions are proposed: (1) The ARN is a two-dimensional network. Climbing and descending aircraft are not considered; (2) The PRDs boundaries mentioned above are being extended and in the non-PRD zone.

Let N represent the ARN to be optimized

$$N = (V, \boldsymbol{D}, \boldsymbol{F}, U, C_N, I_N, T_C) \tag{8}$$

The definitions of the elements in ARN are given as follows.

(1) Here V is the set of ARNNs. There are two kinds of ARNNs: intersection points and airport points. n and m stand for the total number of intersecting points and airports respectively. Then we have

$$V(N) = \{V_1, V_2, \ldots, V_n, V_{n+1}, \ldots, V_{n+m}\} \tag{9}$$

where V_i is an intersecting point if $i \leqslant n$, otherwise it is an airport.

(2) $\boldsymbol{D}$ is a matrix of the route segment lengths between pairs of nodes in the ARN, as given by

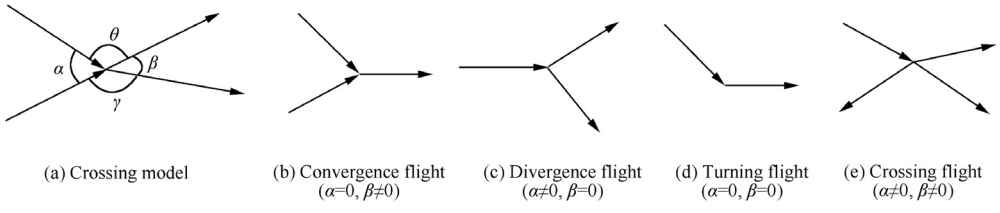

Fig. 2 Diagram of convergence, divergence, turning and crossing flight.

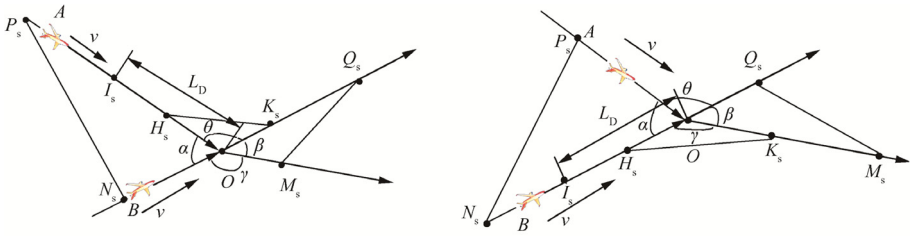

(a) A crossed intersection node O after B (b) A crossed intersection node O before B

Fig. 3 Schematic of crossing route.

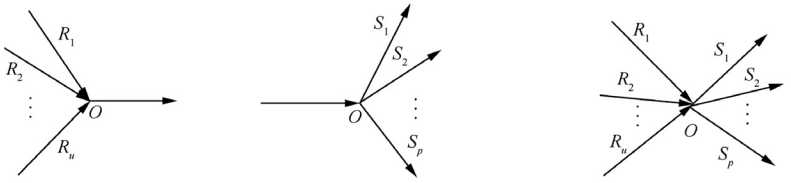

(a) Several routes converge to one route (b) One route diverges into several routes (c) Routes converge at a node and diverge into several routes

Fig. 4 Conflict schematic of intersection nodes of multiple routes.

$$\boldsymbol{D} = \begin{pmatrix} d_{11} & \cdots & d_{1,m+n} \\ \vdots & & \vdots \\ d_{m+n,1} & \cdots & d_{m+n,m+n} \end{pmatrix} \tag{10}$$

where d_{ij} is the actual flying distance between i and j.

(3) $\boldsymbol{F}$ is a matrix of traffic flow

$$\boldsymbol{F} = \begin{pmatrix} f_{11} & \cdots & f_{1,m+n} \\ \vdots & & \vdots \\ f_{m+n,1} & \cdots & f_{m+n,m+n} \end{pmatrix} \tag{11}$$

where f_{ij} indicates the traffic flow from node i to j. f_{ij} depends on the traffic flows between airport pairs and flight routes.

(4) U is the set of PRDs. line (i, j) is a straight-line route segment between node i and j. line (i, j) cannot be intersected with PRDs. Thus,

$$\text{line}(V_i, V_j) \cap U = \varnothing \quad (i \neq j, i > 0, j \leqslant m+n) \tag{12}$$

(5) C_N is the capacity set of ARNNs. As described in Section 2.2, the computational methods of different configurations of ARNN capacity are different. To ensure orderly operation of the ARN, traffic flow must be less than the capacity. Thus, we have

$$f_i < C_{Ni} \quad (i \leqslant n) \tag{13}$$

Given the fact that inflow of a node is equal to outflow of the node, the ARNN flow is one-half of the flow of all route segments connected to this ARNN. The relationship between f_i and f_{ij} is

$$f_i = \frac{\sum_{j=1}^{m+n} f_{ij}}{2} \quad (i \leqslant n) \tag{14}$$

(6) I_N is the set of NSLF which is defined as the ratio of actual distance to the Euclidean distance between ARNNs. The NSLF of a network can be used to measure the convenience of the overall ARN. The larger the NSLF is, the higher the operational costs are and the lower the utilization of the airspace is. I_N can be calculated as

$$I_N = \frac{\sum_{i=1}^{m}\sum_{j=1}^{m} d_{ij}}{\sum_{i=1}^{m}\sum_{j=1}^{m} G_{ij}} \leqslant I_{\max} \quad (i \neq j) \tag{15}$$

where G_{ij} is the Euclidean distance between two nodes i, j; $I_{\max}$ is the maximum NSLF. The typical values of NSLF are 1.4 in a road network[16] and 1.3 in an ARN.

(7) T_C is a surrogate of operation cost measuring the economic performance of the ARN. The lower the value of T_C is, the better the performance of the network is. T_C is defined as

$$T_C = \sum_{i=1}^{n+m}\sum_{j=i+1}^{n+m} f_{ij} d_{ij} \tag{16}$$

The ARN optimization model can be developed as follows. According to regulations that optimize the positions of intersection nodes in a specified area while satisfying safety constraints, the total operation cost of the ARN should be minimum. Here, we present the ARN optimization model as

$$\min \ T_C = \sum_{i=1}^{n+m}\sum_{j=i+1}^{n+m} f_{ij} d_{ij} \tag{17}$$

$$\text{s.t. line}(i,j) \cap U = \varnothing \tag{18}$$

$$f_i < C_{Ni} \tag{19}$$

$$I_N < I_{\max} \tag{20}$$

$$x_{i,\min} \leqslant x_i \leqslant x_{i,\max}, \quad y_{i,\min} \leqslant y_i \leqslant y_{i,\max} \tag{21}$$

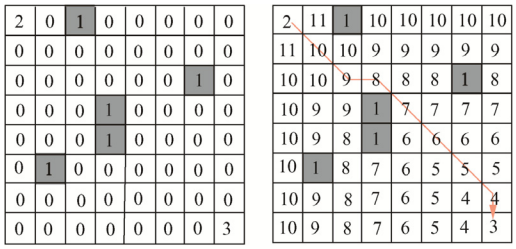

(a) Initial state (b) Final state

Fig. 5 States of cell.

Eq. (17) is the objective function of the model, which minimizes the total operating cost; PRDs restriction, capacity constraints, and NSLF are listed in Eq. (18), (19) and (20) respectively; Eq. (21) gives the boundary of the ARN with x_i and y_i representing the coordinates of V_i. $x_{i,\min}$ and $x_{i,\max}$ are the lateral limits of V_i, while $y_{i,\min}$ and $y_{i,\max}$ are the longitudinal limits of V_i.

4. Algorithm for solving ARN optimization model

4.1. Cellular automata (CA)

A CA consists of a set of cells, cellular space, neighbors, and rules, which can be represented as four tuples as shown in the following[17]:

$$C_A = (S, L_{2D}, N_s, g) \tag{22}$$

Let C_A be the CA system, and S be a set of cellular finite discrete states. At initial time $t = 0$, each ARN cell has two states, 0 and 1. If a cell is a PRD cell, its state is 1, otherwise the state is set to 0. The origin cell status is set to 2, and the state of the destination cell is 3 (Fig. 5(a)). L_{2D} stands for the two-dimensional ARN cellular space. According to ARN model, the entire airspace must be rasterized. N_s represents all neighboring cell states within the airspace. g is a local state transition function that uses the current state of the cell and the state of all its neighbors to determine the evolution of state.

4.1.1. CA evolution

The ARN CA evolution process proceeds as follows. Evolution starts from the cell which is near destination. If the state of the current cell is 0 or greater than 3, then the next state of the cell will be 1 plus the minimum value of its neighbor cells whose states are bigger than or equal to 3. If the state of the current cell is 1, then the state remains unchanged until all the states of its neighbor cells change. (i_c,t) is used to represent the state of the center cell N_c at time t, and (i_n,t) is a state of N_c's neighbor N_n. (i_c,t) can be determined as Algorithm 1.

Algorithm 1. Evolution rules.

```
1 if  {[(ic, t) = 0 or (ic, t) > 3] and (in, t) ⩾ 3}
2     (ic, t + 1) = min[(in, t) ⩾ 3] + 1
3  else
4     (ic, t + 1) = (ic, t)
5 End
```

Based on these rules, the states of each cell after evolution are shown in Fig. 5(b).

4.1.2. CA path optimization

An aircraft starts from a cell near its origin. The state of the cell is greater than 1, and its value is the minimum one among all the neighbor cells. This cell is set as the central cell. Then the aircraft moves to a neighbor cell whose state is less than 1 to the state of central cell. If there are several cells having the same state, the NSLF will be used to choose which cell is connected. The center of the cell is connected to the original cell N_O and to the destination cell N_D with straight lines. For instance, the Euclidean distance between the center of the cell and the original cell is d_1, and the distance to the final cell is d_2. G_{OD} is the distance between N_O and N_D. The NSLF is calculated as $(d_1 + d_2)/G_{OD}$. The cell with the minimum NSLF is chosen as the next cell. Let (i_n, I_n) represent the neighbor cell N_n's NSLF of cell N_c at time t, and (i_n, L_n) be the location of the neighbor cell N_n. We present the following algorithm for path optimization .

Algorithm 2. Path optimization.

```
1 While (t > 0)
2 if {(in, t) = (ic, t) − 1 and min (in, In)}
3    (ic, t − 1) = (in, t)
4    route = [route; (in, Ln)]
5    t = t − 1
6 End
7 End
```

Analogically, path searching continues under NSLF constraints to form the optimal path until the destination is reached. The optimal path is shown as a red solid line in Fig. 5(b). The grey cells marked with 1 are PRD cells; the blank marked with 0 are non-PRD cells; the cells marked with 2 and 3 represent the origin and destination cells respectively. The solid line represents the optimal path.

4.2. ARNN optimization

Given the constraints of ARNNs' capacities in a fragmented airspace, the total cost of the entire air route network can be minimized by merging and moving the intersection nodes.

4.2.1. Merging intersection nodes

Merging nodes could reduce the number of nodes, which in turn alleviates controllers' mental workload, improves airspace safety, and reduces the total cost of entire route network. Based on the capacity constraint in Eq. (19) and the weighted qualitative method, intersection nodes (called as "anchor nodes") with distances less than 100 km can be merged into a single node (called "unknown node").[18] All intersection nodes must meet the capacity constraints after merging. The algorithm is given by

$$P(x,y) = \sum_{i=1}^{N_a}(w_i B_i(x,y)) \Big/ \sum_{i=1}^{N_a} w_i \tag{23}$$

$$w_i = (f_i)^{n_a} \tag{24}$$

where $P(x,y)$ is the coordinate of unknown node, $B_i(x,y)$ the coordinates of anchor node, w_i the weight of anchor node to unknown nodes, n_a the weight coefficient with values between

1 and 3, and N_a the number of anchor nodes. The greater the flow in the anchor nodes is, the greater the effect of the unknown node location is.

Anchor node merging process is shown in Fig. 6. n_1, n_2 and n_3 are three anchor nodes, and f_i is associated segment traffic. The traffic flows of nodes n_1, n_2 and n_3 are $(f_1 + f_2 + f_7 + f_9)/2$, $(f_5 + f_6 + f_8 + f_9)/2$ and $(f_3 + f_4 + f_7 + f_8)/2$ respectively. The three anchor nodes are merged into node n_4 with traffic flow of $(f_1 + f_2 + f_3 + f_4 + f_5 + f_6)/2$.

In the process of merging intersection nodes that satisfy constraints, route segment connection will change, leading to the generation of new intersection nodes. The method described above is therefore repeated until no intersection node is generated. Then the merging process is completed.

4.2.2. Moving intersection nodes

Given the ARNNs capacity constraints in Eq. (19), connected segment traffic is used as the weight, and the intersection nodes are moved to the neighboring cell (excluding the PRDs) with the largest weight. The move is accepted if it satisfies the following two constraints: (1) the total cost of the route network is reduced after moving; (2) both the node and its neighbor nodes satisfy capacity constraints. Otherwise, the intersection nodes remain in their original position. The move is repeated until the solution for the best ARN performance is achieved. But because of the cellular size and the rule limitation, the result is local optimum.

The following rules for ARNN moves are proposed for ARN optimization in fragmented airspace, and be shown in Fig. 7: o represents the intersection node that needs to be optimized. a, b, c, d are adjacent nodes and eight neighbor-cells (1, 2, ... , 8) around the node o. f_i ($i = a, b, c, d$) represents the traffic flow between node o and the adjacent node i.

(1) General rules for node moving.

Step 1. Determine the candidate neighbor-cells which the intersection node will be moved into. Mark the node i with $\max(f_i)$ as Q. Randomly select one as Q if there is more than one node with maximum flow. According to the slope k of the straight line formed by node Q and o, the candidate neighbor-cells can be determined (Fig. 7 (b) and Table 1).

Step 2. Determine the target neighbor-cell Q_c. As shown in Fig. 7(a), according to the relative position of o and Q, one of the candidate neighbor-cells should be selected as the target neighbor-cell which node o will be moved into. For instance, suppose $f_a = \max(f_i)$, and then $Q = a$. According to the range of slope k ($-3 < k < -1/3$) of the line between node Q and o, the candidate neighbor-cells are Cell 3 and Cell 7. Based on the relative position of o and a, Cell 7 is selected as the target neighbor-cell Q_c. Thus, node o will be moved to Cell 7, and is marked as o' without changing its connection status.

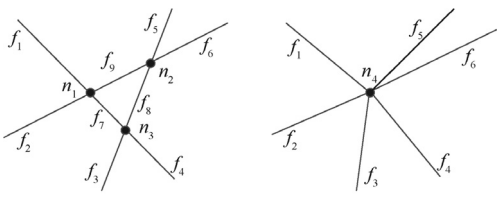

(a) Initial route structure (b) Merging route structure

Fig. 6 Merging intersection nodes.

(2) PRD restrictions. In the process of moving nodes, node o and its neighbor-cells are likely to be in a PRD. If node o is in a PRD, it should be moved to the nearest PRD boundary. Then node o is moved according to the rules described in (1). If the target neighbor-cell Q_c of node o is located in a PRD, two nearest neighbor-cells of Q_c are chosen as the candidate neighbor-cells. Three cases are considered for these two candidate neighbor-cells:

Case 1. If two candidate neighbor-cells are in the PRD, then keep node o unchanged.

Case 2. If one of the two candidate neighbor-cells is in a PRD, then choose the other neighbor-cell as the target neighbor-cell.

Case 3. If none of the two candidate neighbor-cells is in a PRD, then select the candidate which is near the bigger f_i as the target neighbor-cell.

Fig. 7(c) gives an example of moving node with PRD constraints. As it can be seen, Cell 1, shown in a PRD, is one of the neighbor-cells of node o. If $f_b = \max(f_i)$, then Cell 1 is the target neighbor-cell of node o. Since Cell 1 is in a PRD, Cell 2 and 8 will be the new candidate neighbor-cells. If $f_a \geqslant f_c$, then Cell 8 will be the target neighbor-cell. Otherwise, node o will be moved to Cell 2. This cell is marked with o'.

(3) Capacity constraints. Capacity constraints are checked to determine whether to accept moving intersection nodes. We suppose that the adjacent node of node o is p, i.e. $f_p = \max(f_i)$. The following rules are defined.

If node o' and all of its adjacent intersection nodes satisfy capacity constraints, this movement is accepted; Otherwise, this movement is given up. Two neighbor-cells of node Q_c are selected as new candidate neighbor-cells. Then, a new target neighbor-cell is determined based on the rules mentioned in (2). If none of the two new candidate neighbor-cells satisfies capacity constraints, the new candidate neighbor-cells are defined according to rules in (1) and (2) based on traffic flow f_i. If no neighbor-cell can meet capacity constraints, the position of intersection node is kept unchanged.

Here is an example. If $f_b \geqslant f_a \geqslant f_c \geqslant f_d$ in (c), Cell 1 is selected as the target neighbor-cell of node o. However, Cell 1 is in a PRD, and Cell 8 is then selected as the new target neighbor-cell of node o because $f_a \geqslant f_c$. Node o will be moved to Cell 8 and it is marked as o':

Case 1. If the capacity constraints are all satisfied, this movement can be accepted.

Case 2. Otherwise, Cell 2 is reselected as the target neighbor-cell. Node o is moved to Cell 2 and it is marked as o''. If capacity constraints are satisfied, this movement can be accepted; Otherwise, comparing f_a, f_c and f_d, we then define the new target neighbor-cell which satisfies the capacity constraints according to the rules mentioned in (1)–(3).

Case 3. If there is no neighbor-cell which can satisfy capacity constraints, the position of node o is kept unchanged.

(4) Check objective. Under the constraints on capacity and PRDs, target locations of all intersection nodes in the ARN are determined in the next time step based on the rules described above. The CA path optimization

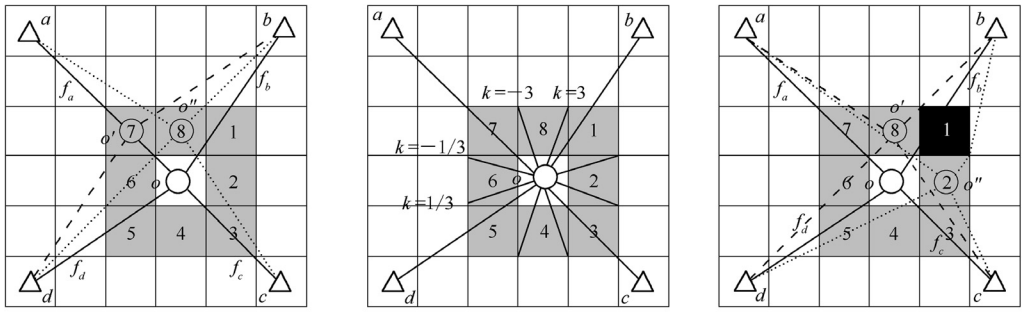

(a) General node movements (b) Relationship of k and alternative neighbor-cells (c) Node movements avoiding three areas

Fig. 7 Node moving rules.

Table 1 Corresponding relationship of slope k and candidate neighbor-cells.

Range of slope k	Candidate neighbor-cells
$1/3 < k < 3$	1, 5
$-1/3 < k < 1/3$	2, 6
$-3 < k < -1/3$	3, 7
$k < -3$ or $k > 3$	4, 8

algorithm is then applied to finding the shortest path between intersection nodes. According to the current flow, the total costs of the current ARN and next ARN, denoted as T_{Cmin} and T_{Co} respectively, are calculated. If $T_{\text{Cmin}} \leqslant T_{\text{Co}}$, the nodes are moved to their target locations. This step is repeated until $T_{\text{Cmin}} > T_{\text{Co}}$. Then the algorithm is terminated, and the optimal ARN is obtained.

5. Case study

In mainland China, there are 9 FIRs namely ZYSH, ZBPE, ZSHA, ZHWH, ZGZU, ZJSY, ZPKM, ZLHW and ZWUQ, as well as 251 PRDs. The airport with the largest traffic flow in each FIR was selected, which are ZYTX, ZBAA, ZSSS, ZHHH, ZGGG, ZJSY, ZPPP, ZLXY and ZWWW (Table A1). These airports are taken as fixed nodes. According to the OD demand between the airports, national ARN optimization is demonstrated here. Fig. 8 depicts the optimization procedures, which is divided into three modules: data collection, optimization model development, and model solution.

Data collection is to extract airspace information and OD demand. First, according to the flight routes and flight-level regulations,[19] 35 routes and the associated location information for each segment between two airports are obtained. The information of PRDs is also retrieved. The current route network is illustrated in Figs. 9 and 10 with solid lines passing through 144 PRDs. The number of air routes passing through PRDs between different airports is given in Table A2. The total length of the current ARN segments is 45507.0 km, and the NSLF is 1.0821.

The average peak-hour traffic volume between airports is calculated based on flight plan in 2014, which is used as OD demand of ARN (Table A2). The total cost of the current ARN is 48304.44 km·acft/h (acft means aircraft).

In the calculation module, the minimum cost of the ARN as expressed in Eq. (17) is taken as the objective function. Four constraints on PRDs avoidance, ARNN capacity, NSLF, and node movement are set up based on Eqs. (18)–(21).

To solve the model, 81 intersection nodes are merged using the algorithm described in Section 4.2.1 until there is no new intersection node generated. In addition, intersection nodes in PRDs are moved to the boundaries of PRDs. The connections of all route segments change as nodes are merged, yielding the initial optimized ARN. The coordinates of intersection node, traffic, and capacity are shown in Table A2. Then the whole airspace is rasterized with at least two grids between the PRDs. The shortest path between each of two airports is searched using the CA algorithms as presented in Section 4.1.

Fig. 9 shows the route optimization schemes of the airspace from ZLXY to ZBAA. ①②③ are the high density areas of intersection nodes that air route between ZLXY and ZBAA must pass through. Around area ①, there are five nodes: CDY, ET, EF, ETH and EFO. After adjustment, the nodes decrease by 3 and the new nodes' locations are (32′) and 32 respectively. Within the scope of ② and ③, the number of nodes decreases from 2 to 1 and from 14 to 2 respectively. After path optimization, node 20 was removed while the position of node 21 is adjusted. Node 35 is the new intersection node generated. Detailed changes of nodes are listed in Table 2. It can be seen from Fig. 9, the original routes (denoted as solid lines) between airport pairs twist in the fragmented airspace, and 13 route segments have passed through 6 PRDs, namely A_{a}, A_{b}, A_{c}, A_{d}, A_{e} and A_{f}. After optimization, as shown by the dotted line, all PRDs are avoided. The route network is optimized in this fragmented airspace. The number of nodes significantly decreases.

ARN within 9 FIRs before and after optimization is shown in Fig. 10. Detailed information is given in Table 3 and Fig. 11. Safety indicators and economic indicators are used to evaluate the ARN performance. Safety indicators are the number of intersection nodes and the number of nodes that pass through PRDs. Economic indicators include the total lengths of route segments, the length of the ARN, the total operational cost of the ARN, and the NSLF. The current routes go through a total of 144 PRDs. The routes between ZPPP and ZSSS, for instance, have to go through 13 PRDs. After optimization, all PRDs are avoided and the operating safety is improved. The number of current ARNNs is 81. After optimization, the number of nodes was greatly decreased by about 50% to 40% (Table A3). The coordination workload between military

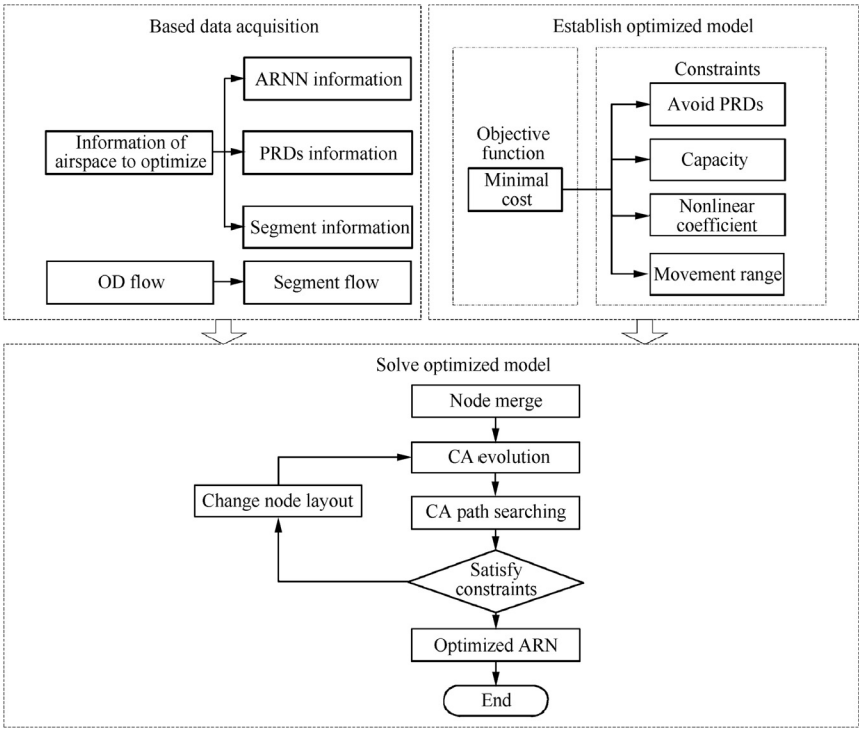

Fig. 8 ARN optimization flowchart.

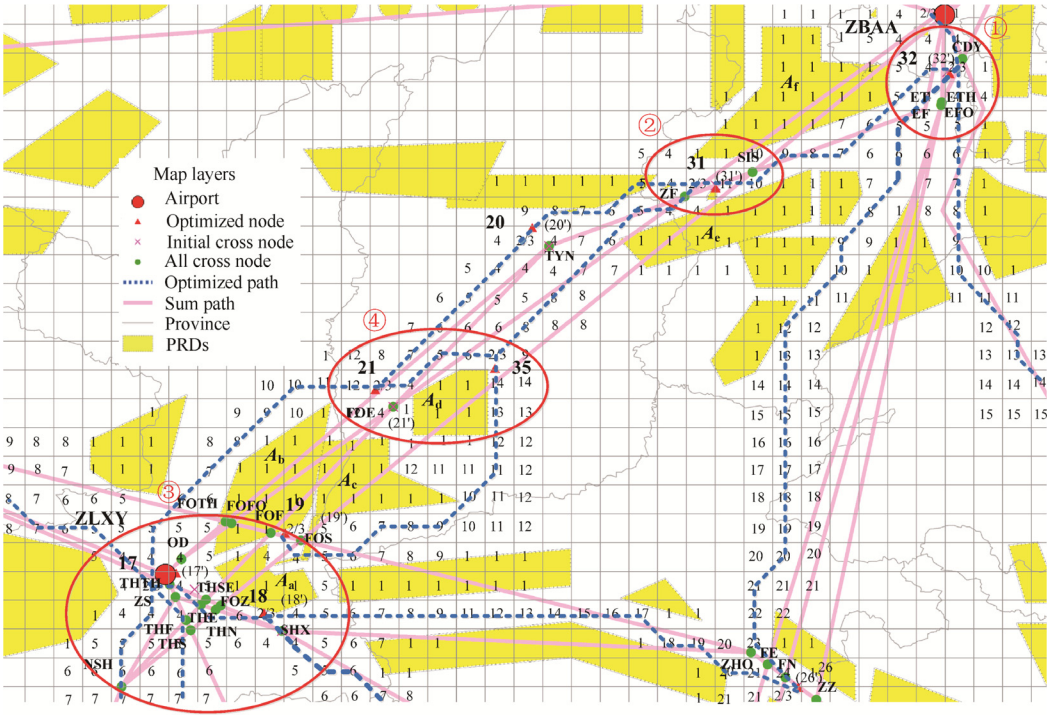

Fig. 9 Route optimization schemes of the airspace from ZLXY to ZBAA.

and civil has been significantly reduced as well as air traffic control (ATC) workload. The total length of all route segments decreased from 45507.0 km to 30929.3 km, a drop of 32.03%. The total length of routes was reduced from 72683.5 km to 68453.88 km, a decrease of 5.82%. The length of ZJSY–ZSSS route decreased by 16.69%, whereas the length of ZPPP–ZGGG route increased by 4.64% due to avoiding PRDs. The total cost of segments declined from 48304.44 km·acft/h to 45308.27 km·acft/h. The ZGGG–ZSSS route cost declined by 16.06%. The NSLF, which changes with the length of the route, decreased by 5.82%. The comparative results on the safety and economic indicators between current

Table 2 ARNN optimization between ZBAA and ZLXY.

No.	Initial node	Coordinate	Number after optimization	Coordinate
①	CDY	E 117°13′27″N 40°34′36″	32	E 116°37′49″N 39°30′01″
	ET	E 116°34′25″N 39°11′42″		
	EF	E 116°34′01″N 39°09′58″		
	EFO	E 116°34′08″N 39°10′31″		
	ETH	E 116°34′25″N 39°11′24″		
②	ZF	E 113°59′04″N 38°14′45″	31	E 114°17′46″N 38°21′33″
	SIS	E 114°40′03″N 38°29′39″		
③	SHX	E 109°55′44″N 33°52′41″	18	E 109°55′44″N 33°52′41″
	THF	E 108°57′47″N 33°59′17″		
	ZS	E 108°51′19″N 34°13′19″		
	THTH	E 108°47′54″N 34°20′44″		
	THSE	E 109°09′48″N 34°11′40″		
	FOTH	E 109°21′39″N 34°58′42″		
	FOFO	E 109°25′17″N 34°57′48″		
	FOF	E 109°48′56″N 34°51′56″		
③	NSH	E 108°18′50″N 33°19′13″	17	E 109°02′56″N 34°17′49″
	THS	E 109°00′33″N 33°53′12″		
	THE	E 109°06′39″N 34°08′26″		
	THN	E 109°15′42″N 34°05′31″		
	FOZ	E 109°18′43″N 34°07′59″		
	OD	E 108°54′59″N 34°36′01‴		
④	FOE	E 111°02′56″N 36°08′03″	21	E 110°52′10″ N36°18′19″
			35(new node)	E 112°04′34″ N36°32′02″

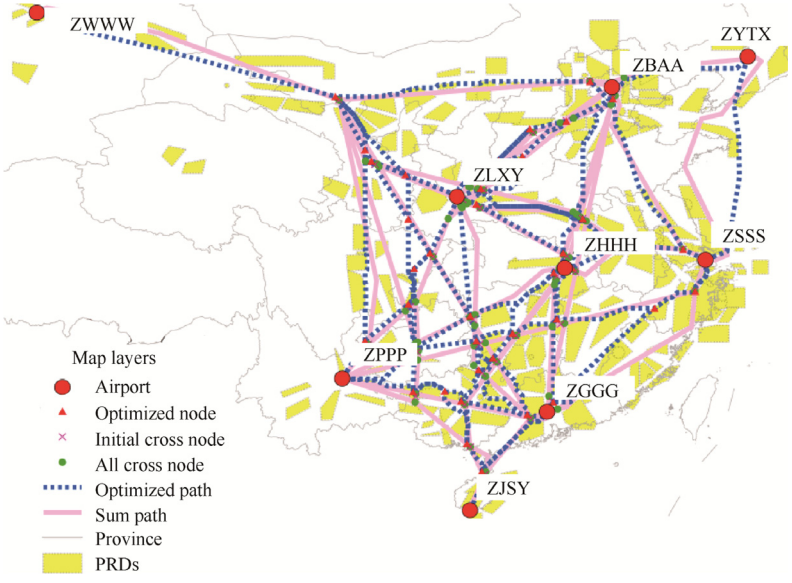

Fig. 10 ARN optimization chart.

ARN and optimized ARN are presented in Fig. 11. The lengths of ZPPP–ZJSY, ZPPP–ZGGG, ZGGG–ZHHH, ZLXY–ZJSY and ZBAA–ZYTX were increased by 8.09%, 4.64%, 2.86%, 1.04% and 8.25% in order to avoid PRDs. However, the lengths and cost of the other 30 routes are less than those of the current routes.

6. Conclusions

An ARN optimization model is proposed here based on the capacities of ARNNs while avoiding PRDs in the fragmented airspace. To solve the model, a CA algorithm is developed, and solution procedure is presented in detail. Computational results of 35 routes in mainland China show that the total operational cost of the ARN, the number of routes that pass through PRDs, and the number of nodes are all drastically reduced after optimization. It is demonstrated that the proposed method can be used for planning and design of fragmented ARNs to improve the economy and safety of ARNs. The properties of complex networks and the dynamics shall be introduced into ARN optimization problems in future studies.

Table 3 Comparative results on ARN performance before and after optimization.

Type	Indicator	Current ARN	Optimized ARN	Change (%)
Safety	Number of nodes	84	49	−41.67
	Total number of air routes passing through PRDs	144	0	−100
	Number of air routes passing through PRDs between ZPPP and ZSSS	13	0	−100
Economy	Total length of segments (km)	45507.0	30929.3	−32.03
	Total length of route (km)	72683.5	68453.88	−5.82
	Length of ZJSY-ZSSS route (km)	2093.65	1744.22	−16.69
	Total ARN cost (km·acft/h)	48304.44	45308.27	−6.22
	ZGGG-ZSSS ARN cost (km·acft/h)	3068.68	2575.69	−16.06
	ARN NSLF	1.0821	1.0189	−5.82

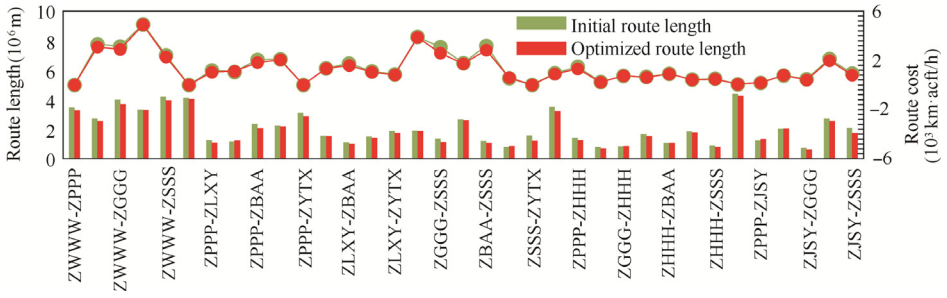

Fig. 11 Comparative results on ARN before and after route optimization.

Acknowledgements

This research was co-supported by the National Natural Science Foundation of China (No. 61304190), the Natural Science Foundation of Jiangsu Province (No. BK20130818), and the Fundamental Research Funds for the Central Universities of China (No. NJ20150030).

Appendix A

Table A1 Airport code.

Chinese name	Wulumuqi/ Diwobao	Shenyang/ Xiantao	Guangzhou/ Baiyun	Kunming/ Changshui	Shanghai/ Hongqiao	Xi'an/ Xianyang	Beijing/ Capital	Wuhan/ Tianhe	Sanya/ Fenghuang
Four words	ZWWW	ZYTX	ZGGG	ZPPP	ZSSS	ZLXY	ZBAA	ZHHH	ZJSY

Table A2 Traffic between airports.

Airport pair	Traffic (acft/h)	PRDs No.	Airport pair	Traffic (acft/h)	PRDs No.
ZWWW-ZPPP	0	6	ZWWW–ZLXY	7.292	3
ZWWW-ZGGG	4.706	6	ZWWW-ZBAA	8.865	10
ZWWW–ZSSS	3.455	5	ZWWW-ZYTX	0	10
ZPPP-ZLXY	5.712	0	ZPPP-ZGGG	5.467	6
ZPPP-ZBAA	5.239	3	ZPPP-ZSSS	5.618	13
ZPPP-ZYTX	0.009	7	ZLXY-ZGGG	5.323	2
ZLXY-ZBAA	9.349	1	ZLXY-ZSSS	4.417	1
ZLXY-ZYTX	2.812	5	ZGGG-ZBAA	12.400	6
ZGGG- ZSSS	13.638	6	ZGGG-ZYTX	3.971	6
ZBAA- ZSSS	16.013	2	ZBAA-ZYTX	4.126	0
ZSSS-ZYTX	0.008	3	ZWWW-ZHHH	1.641	4
ZPPP-ZHHH	6.275	2	ZLXY-ZHHH	1.929	0
ZGGG-ZHHH	5.223	0	ZJSY-ZHHH	2.394	2
ZHHH-ZBAA	5.110	3	ZHHH-ZYTX	1.427	3
ZHHH- ZSSS	3.455	0	ZWWW-ZJSY	0.097	9
ZPPP-ZJSY	0.849	4	ZLXY-ZJSY	2.285	4
ZJSY-ZGGG	3.916	1	ZJSY-ZBAA	4.664	5
ZJSY-ZSSS	2.714	6	ZJSY-ZYTX	0	0

Table A3 Node information after optimization.

No.	Longitude	Latitude	Traffic (acft/h)	Capacity (acft/h)	Longitude after optimization	Latitude after optimization
1	E 102°46′39″	N 39°25′12″	4.342	23.405	E 102°35′48″	N 39°35′21″
2	E 104°35′53″	N 36°06′23″	2.849	26.415	E 104°25′02″	N 36°16′43″
3	E 104°16′48″	N 26°51′42″	1.827	34.449	E 104°05′46″	N 27°02′27″
4	E 106°24′25″	N 28°48′48″	1.843	32.235	E 106°17′29″	N 28°56′11″
5	E 106°45′15″	N 26°28′40″	2.379	34.417	E 106°35′09″	N 26°38′25″
6	E 106°39′46″	N 24°11′18″	1.449	34.896	E 106°31′56″	N 24°25′27″
7	E 109°09′14″	N 23°46′33″	2.088	34.965	E 108°58′07″	N 23°56′37″
8	E 109°25′58″	N 21°35′06″	1.715	35		
9	E 110°10′44″	N 20°08′34″	2.819	34.095	E 110°00′46″	N 20°18′46″
10	E 112°29′05″	N 23°04′07″	2.583	17.933	E 112°18′55″	N 23°14′58″
11	E 110°01′32″	N 25°22′56″	2.064	32.341	E 109°51′08″	N 25°32′44″
12	E 110°45′41″	N 25°58′27″	1.961	33.815	E 110°34′30″	N 26°09′35″
13	E 109°54′24″	N 26°51′19″	2.608	34.718	E 109°44′42″	N 27°02′27″
14	E 109°35′21″	N 28°08′09″	2.717	34.999	E 109°25′26″	N 28°19′20″
15	E 111°44′36″	N 27°19′02″	2.113	35	E 111°33′56″	N 27°24′52″
16	E 107°33′33″	N 31°22′00″	2.992	34.999	E 107°23′21″	N 31°33′10″
17	E 109°02′56″	N 34°17′49″	7.028	35	E 108°51′42″	N 34°27′47″
18	E 109°55′44″	N 33°52′41″	1.331	34.909	E 109°44′42″	N 34°03′45″
19	E 110°07′08″	N 34°47′25″	0.577	30.007	E 109°57′33″	N 34°51′49″
20	E 112°37′08″	N 37°44′57″	2.431	32.209	E 112°26′57″	N 37°56′02″
21	E 111°02′56″	N 36°08′03″	1.341	35		
22	E 114°00′03″	N 27°53′06″	4.535	35	E 113°48′52″	N 28°09′44″
23	E 113°49′58″	N 30°22′05″	3.093	34.687	E 113°39′14″	N 30°22′18″
24	E 114°18′53″	N 31°23′18″	2.462	34.963	E 114°08′09″	N 31°33′10″
25	E 114°45′51″	N 30°36′03″	3.304	34.999	E 114°35′27″	N 30°46′43″
26	E 115°07′22″	N 33°19′30″	5.907	33.025	E 115°07′35″	N 33°18′54″
27	E 116°58′36″	N 31°59′17″	1.888	24.894	E 117°00′01″	N 31°58′48″
28	E 120°11′25″	N 31°44′30″	4.557	27.767	E 120°12′47″	N 31°44′23″
29	E 120°48′53″	N 29°35′56″	3.662	34.201	E 120°49′44″	N 29°34′38″
30	E 115°29′52″	N 40°23′21″	1.477	34.473	E 115°30′04″	N 40°21′48″
31	E 114°17′46″	N 38°21′33″	2.901	35	E 114°17′47″	N 38°20′04″
32	E 116°37′49″	N 39°30′01″	12.331	35	E 116°39′08″	N 39°28′57″
33	E 113°36′27″	N 23°54′23″	6.324	26.198	E 113°37′37″	N 23°53′25″
34	E 114°50′58″	N 24°16′59″	2.725	35		
35			1.962	32.152	E 112°04′34″	N 36°32′02″
36			4.321	34.561	E 106°08′42″	N 35°35′39″
37			1.856	34.234	E 108°08′31″	N 24°27′36″
38			2.342	21.231	E 106°35′42″	N 30°49′47″
39			1.215	31.203	E 106°20′59″	N 33°13′00″
40			2.512	34.233	E 104°06′00″	N 36°51′32″
41			3.662	34.201	E 118°45′36″	N 28°44′44″
42			3.093	34.687	E 111°49′48″	N 28°58′00″
43			2.865	34.577	E 104°04′37″	N 37°41′49″

Notes: 35–43 are new nodes.

References

1. Zeinali M, Rutherford D, Kwan I, Kharina AUS. *Domestic airline fuel efficiency ranking*. Washington, D.C.: International Council on Clean Transportation; 2013.
2. Du WB, Zhou XL, Lordan O, Wang Z, Zhao C, Zhu YB. Analysis of the Chinese airline network as multi-layer networks. *Transport Res Part E: Logist Transport Rev* 2016;**89**:108–16.
3. Cong W, Hu MH, Dong B, Wang YJ, Feng C. Empirical analysis of airport network and critical airports. *Chin J Aeronaut* 2016;**29**(2):512–9.
4. Zhang J, Cao XB, Du WB, Cai KQ. Evolution of Chinese airport network. *Phys A: Stat Mech Appl* 2010;**389**(18):3922–31.
5. Zhao S, Zhang XJ, ZHU YB, Cai KQ. A methodology for designing transition route network between en-route airspace and terminal areas. *Proceedings of the IEEE/AIAA 27th digital avionics systems conference*; 2008 Oct 26-30; St. Paul (MN), USA. Piscataway (NJ): IEEE Press;2008.
6. Rivière T. Redesign of the European route network for sector-less. *Proceedings of the 23rd digital avionics systems conference*; 2004 Oct 28; Piscataway (NJ): IEEE Press;2004.
7. Cai KQ, Zhang J, Zhou C, Cao XB, Tang K. Using computational intelligence for large scale air route networks design. *Appl Soft Comput* 2012;**12**(9):2790–800.
8. Du WB, Gao Y, Liu C, Zheng Z, Wang Z. Adequate is better: Particle swarm optimization with limited-information. *Appl Math Comput* 2015;**268**(1):832–8.
9. Du WB, Ying W, Yan G, Zhu YB, Cao XB. Heterogeneous strategy particle swarm optimization. *IEEE Trans Circ Syst II: Exp Briefs* 2016;**64**(4):467–71.
10. Jin C, Zhu YB, Fang J, Li YT. An improved methodology for ARN crossing waypoints location problem. *Proceedings of the 31st*

digital avionics systems conference (DASC); 2012 Oct 14-18; Williamsburg (VA), USA. Piscataway (NJ): IEEE Press; 2012.
11. Chen CL. Research on optimization method based on complex network for crossing waypoints location [dissertation]. Hefei: University of Science and Technology of China; 2011 [Chinese].
12. Xu YC, Zhu YB. Methodology of key network nodes optimization and restricted airspace avoiding. *J Civil Aviation Univ China* 2013;**31**(1):41–5 [Chinese].
13. Wang SJ, Gong YH. Research on air route network nodes optimization with avoiding the three areas. *Safety Sci* 2014;**66**:9–18.
14. Zhou J. Research of the airspace en-route network based on the Bi-level programming [dissertation]. Nanjing: Nanjing University of Aeronautics and Astronautics; 2008 [Chinese].
15. Zhou W. Research on terminal area air traffic evaluation and planning method [dissertation]. Xi'an: Northwestern Polytechnical University; 2007 [Chinese].
16. Ministry of Construction of the People's Republic of China. Code for transport planning on urban road. Beijing: Standards Press of China; 1995. Report No.: GB 50220-95 [Chinese].
17. Jia B, Gao ZY, Li KP. *Models and simulation of traffic system on the theory of cellular automaton*. Beijing: Science Education Press; 2007. p. 11–7 [Chinese].
18. Civil Aviation Administration of China. Rules of air traffic management of Civil Aviation Administration of China. Beijing: Civil Aviation Administration of China; 1999. Report No.: CCAR-93TM-R3 [Chinese].
19. Chinese People's Air Army Headquarters Standard. Facility regulation of the flight routes and levels of Chinese international and domestic flights. Beijing: Chinese People's Air Army Headquarters; 2009. [Chinese].